Chemical Physics Letters 726 (2019) 57–61

Contents lists available at ScienceDirect

Chemical Physics Letters

journal homepage: www.elsevier.com/locate/cplett

Research paper

First-principles study of V-decorated porous graphene for hydrogen storage

Lihua Yuan[a,b,*], Daobin Wang[b], Jijun Gong[b], Cairong Zhang[a,b], Liping Zhang[b], Meiling Zhang[b,c], Xiaojuan Wu[a], Long Kang[a]

[a] State Key Laboratory of Advanced Processing and Recycling of Non-Ferrous Metals, Lanzhou University of Technology, Lanzhou 730050, China
[b] School of Sciences, Lanzhou University of Technology, Lanzhou 730050, China
[c] School of Nuclear Science and Technology, Lanzhou University, Lanzhou 73000, China

HIGHLIGHTS

- To avoid clustering among V atoms, PG unit cell should contain two V atoms.
- Four H_2 are adsorbed around a V atom with the adsorption energy of -0.564 eV/H_2.
- Ab initio MD simulation shows six H_2 can be adsorbed on both sides of V-PG at 300 K.
- At 300 K and without external pressure, the hydrogen storage capacity is 4.58 wt%.

ARTICLE INFO

Keywords:
Porous graphene
Hydrogen storage
Ab initio MD
First-principles

ABSTRACT

Hydrogen storage capacity on vanadium (V) decorated porous graphene (PG) has been studied using first-principles calculations. The results show, to avoid a tendency of clustering among V atoms, the maximum number of adsorbed V atoms is two for both sides of the PG unit cell, and four H_2 molecules can be adsorbed around each V atom. Furthermore, at 300 K and without external pressure, ab initio molecular-dynamics simulations results show that six H_2 molecules can be stably adsorbed on both sides of unit cell of PG decorated with V atoms with the gravimetric hydrogen storage capacity of 4.58 wt%.

1. Introduction

Due to its high efficiency, harmlessness and renewable, hydrogen energy is one of the promising alternative green energy sources. However, it is still a challenge to design solid state hydrogen storage materials with high gravimetric and volumetric densities near ambient temperature conditions [1,2]. Carbon-based nanomaterials such as graphene have been designed and widely studied for hydrogen storage due to their high surface-volume ratio and light weight [2–4]. However, hydrogen adsorption on these pristine carbon-based materials is only through weak van der Waals forces, hence the adsorption energies of hydrogen are very low, resulted in decreasing the hydrogen storage capacity [5]. To improve the hydrogen adsorption ability of carbon materials, many studies have been devoted to decorate the carbon materials with alkaline metal atoms [6–8], alkaline earth metal atoms [9–12] and transition metal atoms (TM) [13–17]. Many researchers [7,8,18] have thought that Li-decorated graphene can serve as a high-capacity hydrogen storage medium, but, the adsorption of H_2 are still weak. Very recently, Fay et al. [15] have studied hydrogen storage properties of Nb-decorated graphene.

Porous graphene is a collection of graphene-related materials with nanopores in the plane, which exhibits novel properties different from those of pristine graphene. It owns many good features including light weight, large surface area and high porosity. In recent years, the application of porous graphene in hydrogen storage has gained more and more attention from researchers. For the first time, Bieri and his co-workers [19] have synthesized the regular two dimensional porous graphene (PG), benzene ring is periodically missing in graphene plane, the distance between the nanopores is 7.4 Å, and the PG unit cell consists of two C_6H_3 rings. Then, the electronic properties of the PG have been studied by density function theory [20] and crystal orbital methods [21] in detail. The existence of nanopores may be helpful for separation of metal atoms adsorption on PG, avoiding the metal clustering.

Some works [20,22,24–30] have studied hydrogen storage capacity of metal-decorated PG based on Bieri's structure. Du et al. [20] have studied hydrogen storage capability of Li-decorated PG by VASP code, the binding energy for a Li atom on PG is much stronger than that on

* Corresponding author at: School of Sciences, Lanzhou University of Technology, Lanzhou 730050, China.
E-mail address: yuanlh@lut.cn (L. Yuan).

https://doi.org/10.1016/j.cplett.2019.04.026
Received 17 December 2018; Received in revised form 3 April 2019; Accepted 10 April 2019
Available online 11 April 2019
0009-2614/

pristine graphene, and the hydrogen storage capacity is 12 wt% with the average adsorption energy of 0.243 eV/H_2. Ao et al. [22] have investigated hydrogen storage capacity of Al-decorated PG using $Dmol^3$ code with Local density approximation (LDA) functional and DFT-D method, six H_2 molecules can be adsorbed around each Al atom. They have thought the overestimate of the binding energy by LDA functional can compensate the van der Walls interactions [23], whereas DFT-D method has considered the van der Walls forces, so the adsorption energy of H_2 is maybe overestimated. Furthermore, the effect of oxygen atom doping on hydrogen storage capability of Li-decorated PG has been investigated by SIESTA code [25]. Lu et al. [26] have reported that boron (B) doping on PG can effectively enhance the interaction between metal atoms and the PG, but nitrogen doping weaken the interaction. And they have found doping of B atoms on PG can increase the adsorption energy of H_2 molecules on Ca-decorated PG, but slightly decrease the adsorption energy of H_2 molecules on Li-decorated PG. While Wang et al. [27] reported that nitrogen doping on PG can enhance the binding energy of Li atoms.

There is a little study on hydrogen storage properties of TM decorated PG. We have studied the hydrogen storage ability of PG decorated with TM (Y, Ti and Sc) [28–30]. Based on our previous studies, we investigate the adsorption of hydrogen on vanadium (V) decorated PG in this paper. First, the stable adsorption site of V atoms and the maximum number of adsorbed V atoms on PG unit cell is discussed. Then, the adsorption ability of H_2 molecule on the V-PG system is discussed by analyzing geometric structures of H_2 adsorbed on V-PG, the adsorption energies of H_2, the projected density of states, and the electron density difference. Finally, the stability of hydrogen adsorption system at ambient temperature is tested by ab initio molecular-dynaics (MD) simulation.

2. Method of calculation

We have performed calculations based on Density Functional Theory using the Cambridge serial total energy package (CASTEP) [31]. The ultrasoft pseudopotentials is adopted, and the exchange-correlation interaction between electrons has been described by generalized gradient approximation (GGA) with the scheme of PBE functional [32]. As we all know, the GGA method underestimates the binding energy. To improve the computational precision, dispersion-corrected density function theory (DFT-D) method in the Grimme scheme [33] has been used in all the calculations, which is tested and verified in our previous work [28]. The energy cutoff and the k-mesh grids have been tested to confirm the convergence of our calculations (see Fig. S1). Considering the computational cost, the cutoff energy for the plane-wave basis set is chosen to be 500 eV, and the k-mesh grids are 6 × 6 × 1 for the PG cell. The spin-polarized calculations are performed, and all atoms are allowed to relax in calculations. The structures are fully optimized without any symmetry constraints, the maximum force on each atom is 0.01 eV/Å, and the energy convergence tolerances is 5.0×10^{-6} eV per atom. The convergence threshold is set to 1.0×10^{-6} eV/atom in the self-consistent field (SCF) calculations. The unit cell of PG is used in the calculation with periodic boundary conditions, the optimized lattice parameters of the unit cell are a = b = 7.49 Å, which are closely consistent with the Bieri's experimental value [19] and some theoretical value [20,24,34,35], and a vacuum of 18 Å is employed along the direction of the PG sheet.

The average binding energies of V atom adsorbed on the PG is calculated as following equation

$$E_b = [E_{nV+PG} - E_{PG} - nE_V]/n \quad (1)$$

where E_{nV+PG} is the total energy of the system with n V atom adsorbed on the PG layer, E_{PG} is the total energy of PG sheet, and E_V is the total energy of an isolated V atom, n is the number of V atoms.

For the case of single side of V-PG system, the adsorption energy and average adsorption energy of H_2 molecules on V-decorated PG system is defined as

$$E_{ad} = \left[E_{nH_2+V+PG} - E_{(n-1)H_2+V+PG} - E_{H_2}\right] \quad (2)$$

$$\bar{E}_{ad} = \left[E_{nH_2+V+PG} - E_{V+PG} - nE_{H_2}\right]/n \quad (3)$$

where E_{nH_2+V+PG}, $E_{(n-1)H_2+V+PG}$, E_{V+PG} and E_{H_2} denote the total energy of the V-decorated PG system with n H_2 molecules adsorbed, the total energy of the system with (n − 1) H_2 molecules adsorbed, the total energy of V-decorated PG system and the total energy of free H_2 molecule, respectively.

3. Results and discussion

3.1. Electronic structure of V-decorated PG

First, we investigate the electronic and structural stability of a V atom adsorbed on PG. There are two kinds of carbon atoms in PG unit cell, C1 atoms are connected with two carbon atoms and one hydrogen atom, and C2 atoms are connected with three carbon atoms. We consider six high symmetry adsorption sites for a V atom on the single side of PG (see Fig S2), which are the center site above the C hexagon (h), the center site above the C-H hexagon near the porosity (h0), the bridge site over C1-C2 bond (b1), the bridge site over C2-C2 bond (b2), the top site directly above C1 atom (t1), and the top site directly above C2 atom (t2), respectively. No matter where the V atom is initially placed, it always moves to h or b2 site after relaxation. The V atom more prefers to adsorb on the h site of PG by further analyzing the binding energies, as shown in Table S1.

Fig. 1(a) describes the optimized geometry structure of a V atom decorated PG, the distance between a V atom and the center of C hexagon in PG layer is 1.518 Å. By analyzing the Mulliken populations, we find that the V atom has positive charge of 1.40 e as a V atom approaching to PG sheet, while all carbon atoms are negatively charged. Therefore, the electron potential difference causes an electronic field between the positively charged V and negatively charged C atoms, leading to enhance the interaction between V and PG. Fig. 1(b) shows the significant changes of the total DOS of the PG sheet after adsorption of a V atom, the DOS peaks of PG shift to lower energy after a V atom is adsorbed, namely, electrons tend to occupy low levels, which proves high stability for V-PG system. And it can be further observed that the changes of the total DOS near Fermi surface mainly comes from the contribution of 3d orbital of a V atom, the V 4s orbital electrons are almost located above the Fermi energy level, that is, the occupied 4s orbital becomes a non-occupied state after a V atom adsorbs on PG.

To examine denser coverage of V atoms on PG, the second V atom is initially set above the other center of C hexagon of the PG on the same side, two V atoms automatically move to the top sites of the C2 atom

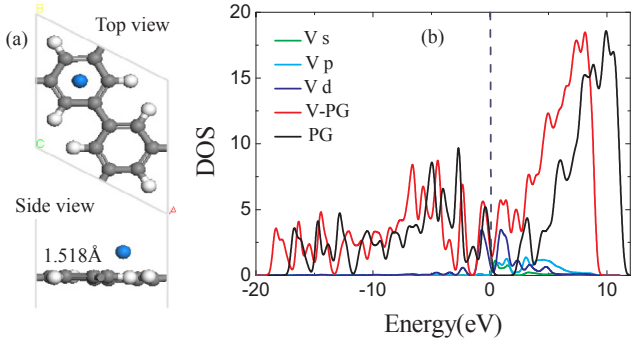

Fig. 1. (a) The optimized geometry structure of a V atom decorated PG. The gray, white and blue ball in this and following figures denote C, H and V atoms, respectively. (b) Total DOS of PG and V-PG system, and the PDOS of V s, p and d orbital.

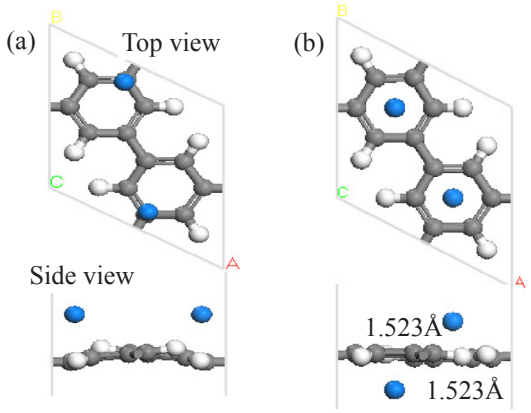

Fig. 2. The optimized geometry structure of two V atoms adsorbed on single side and double sides of PG.

Table 1
The average adsorption energies ($\bar{E}_{ad}$) and adsorption energies (E_{ad}) of H_2 molecules on the single side of V-PG system. L_{av} is the average bond length of n H_2 molecules.

Number of H_2	1	2	3	4
$\bar{E}_{ad}$ (eV)	−0.731	−0.761	−0.736	−0.564
E_{ad} (eV)	−0.731	−0.791	−0.685	−0.049
L_{av} (Å)	0.851	0.843	0.836	0.815

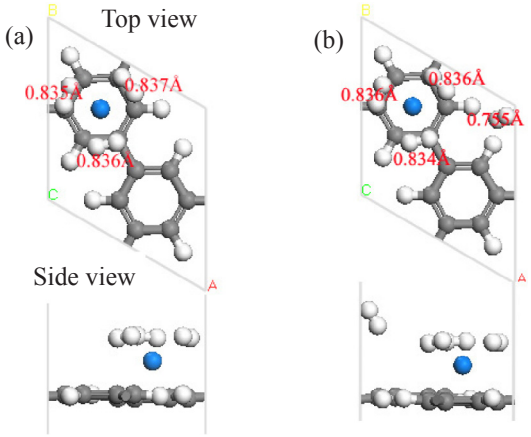

Fig. 3. The optimized geometry structure of the V-PG with three H_2 (a) and four H_2 (b) adsorption. Red digits represent the corresponding bond length of H-H.

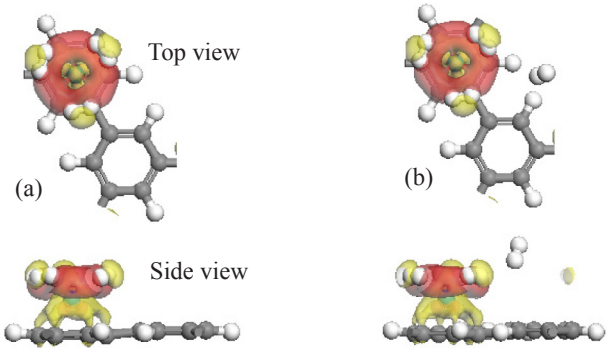

Fig. 4. The charge density differences of n H_2 adsorbed on V-PG system for n = (a) 3 and (b) 4. The red and yellow colors represent electron accumulation and depletion regions. The isovalue is taken to be 0.025 e/Å^3. (For interpretation of the references to colour in this figure legend, the reader is referred to the web version of this article.)

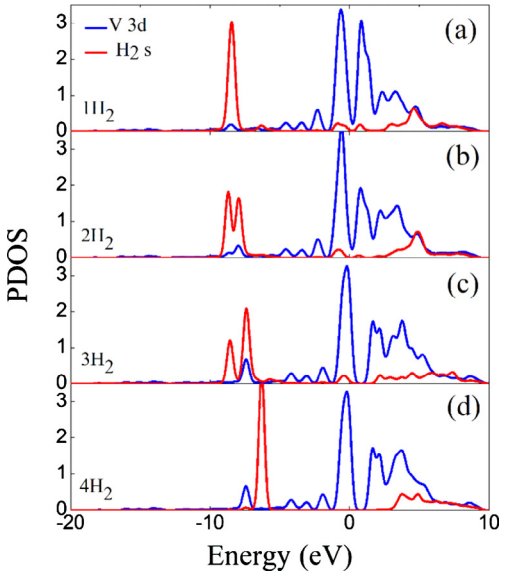

Fig. 5. Partial density of states of H_2 1s (red curve) and V 3d (blue curve) orbitals for adsorption 1–4 H_2 molecules in V-PG system. (For interpretation of the references to colour in this figure legend, the reader is referred to the web version of this article.)

after relaxation, the optimized geometry structure is shown in Fig. 2(a). For better demonstrating the position of two V atoms on PG, (2 × 2) supercell of the PG is shown in Fig. S3, and V atom bonds with its nearest V atom with the bond length of 1.751 Å. To avoid the V atoms clustering, the only one V atom should be contained in the single side of PG unit cell. For the case of two V atoms on double-sided PG, the stable geometry configuration of two V atoms decorated PG unit cell is shown in Fig. 2(b). A slight deformation can be seen, each V atom has a charge of + 1.31 e, and the average binding energy is −4.423 eV. The distance between each V atom and the center of hexagon in PG layer is 1.523 Å.

3.2. Adsorption of H_2 molecules on V-decorated PG

A details theoretical investigation of H_2 adsorption on single side of V-PG system is discussed firstly. The average adsorption energies, adsorption energies and the average bond length of hydrogen molecules on the single side of V-PG system are summarized in Table 1. The first H_2 molecule prefers to adsorb on C atom and tend to tilt toward V atom with adsorption energy of −0.731 eV, and the bond length of H-H is elongated to 0.851 Å (Fig. S4). By analyzing Mulliken population, each hydrogen atom carries negative charge of −0.20 e and −0.11 e, and V is positively charged with charge of 1.40 e, which indicates electrons transfer from V atom to H atom, and the covalent bond of H_2 molecule becomes polarized and ionic bonding forms through attractive Coulomb interaction between negatively charged H and positively charged V. No matter where the second H_2 is initially placed, the two H_2 molecules are symmetrically on both sides of the V atom after relaxation (Fig. S4). To our surprise, when the third H_2 molecule is placed, three H_2 molecules are parallel to the PG plane after relaxation. No matter how we adjust the position of the three H_2 molecules, the optimized geometry structure of system is still consistent with that of the Fig. 3(a), and each hydrogen atom of H_2 molecules carries negative charge of 0.14 e by analyzing Mulliken population. No matter where the fourth H_2 molecule is initially placed, the positions of the three previously adsorbed H_2 molecules on the V-PG remain unchanged, and the fourth H_2 molecule is weakly adsorbed by the V atom with adsorption energy of −0.049 eV and bond length of 0.755 Å (the bond length of free H_2 is 0.753 Å that is consist with the report in reference [24]). If more H_2 molecules are further increase, the H_2 molecules always like to occupy the other C hexagone without V adsorption and the bond length of H-H is not

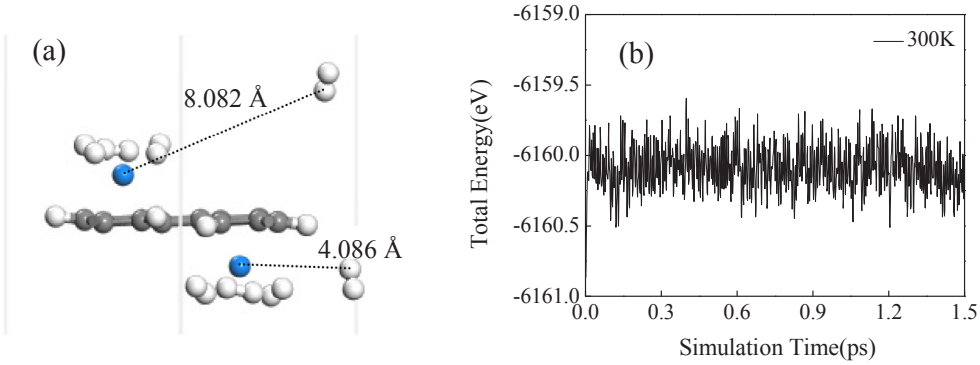

Fig. 6. The equilibrated structure of the $8H_2$-V-PG (a) and fluctuations of total energy as a function of simulation time (b) in ab initio MD simulations at 300 k.

elongated, which belong to physisorption.

In order to have an illuminating insight into the nature of H_2 molecules adsorption on the V-PG system, the charge density difference for the H_2 molecules adsorbed on V-PG system is shown in Fig. 4 and Fig. S5. We can observed depletion of charges between the two H atoms of the H_2 molecule, which correspond to the σ orbital of H_2, and the accumulation of charges around the H_2 molecule, which is relevant to the σ^* orbital of H_2. This phenomenon reflects the strong Kubas interaction [36], the filled H_2 σ orbital transfers electrons to the V empty 3d orbital, conversely, V back-donates electrons to the H_2 σ^* orbital, the adsorption mechanism of H_2 molecules on V-PG has similarities to that of the Ti-decorated graphene system [37]. The feedback bond forms by the transfer of 3d electrons of V atoms to σ^* orbital of H_2 molecules, which plays a very important role for H_2 molecules strongly adsorbed on V-PG system. Fig. S5(b) shows the charge accumulation between two adsorbed H_2 molecules, which also illustrates the interaction between the H_2 molecules and induce an enhancement of the adsorption energy of the second H_2 molecule. Fig. 4(a) shows the charges distribute uniformly among H_2 molecules, this means that three H_2 molecules are strongly adsorbed around the V atom. From Fig. 4(b), it can be observed that there is no charges distribution around the fourth H_2, which indicates the fourth H_2 molecule is weakly adsorbed by the V atom, and the result is consistent with the conclusion judged by the adsorption energy of the fourth H_2 molecule.

The partial density of states (PDOS) of H_2 1s and V 3d orbitals further gives information of interaction between H_2 molecules and the V atom, as shown in Fig. 5. When the first H_2 molecules adsorbed on V-PG, there are overlap between the H_2 σ^* (σ) orbital and V 3d orbital at -0.6 eV (-8.5 eV). This phenomenon reflects the Kubas interaction. When the second H_2 molecule is adsorbed, band broadening of H_2 molecules level indicates H_2-H_2 interaction, and the interaction increases adsorption energies of H_2 molecules in turn, so the adsorption energy of the second H_2 molecule is lower than that of the first H_2 molecule (see Table 1). The main peak of H_2 σ orbital moves to the right (From -8 eV to -7.4 eV) with the third H_2 molecule adsorbed, which indicates the interaction between H_2 and V-PG begins to weaken with increasing of H_2 molecules. After the fourth H_2 molecule adsorbed on V-PG, the main peak of H_2 σ orbital continues to move to the right, and there are no obvious peak overlap of the H_2 σ (or σ^*) orbital and V 3d orbital below Fermi level, which indicates very weak interaction between the fourth H_2 molecule and a V atom. From Table 1, the adsorption energy of the fourth H_2 molecule is -0.049 eV, indicating weak adsorption, while the average adsorption energy of four H_2 molecules is -0.564 eV, indicating strong adsorption. The fourth hydrogen molecule is weakly adsorbed on the V-PG system through the above analysis. So, to determine whether the nth H_2 molecule can be strongly adsorbed by the system, the adsorption energy of H_2 molecules is more accurate than the average adsorption energy.

For the case of H_2 molecules adsorbed on double sides of PG decorated with two V atoms, the H_2 molecules are inclined to be parallel on the PG, the relaxation configurations are shown in Fig. S6. Eight H_2 molecules at most can be adsorbed on V-PG, the interaction between H_2 molecules and V-PG system become weaker with more H_2 molecules increasing. The adsorption energies of H_2 molecules are listed in Table S2.

In order to test the stability of H_2 molecules on the V-PG system at ambient temperature, ab initio MD as implemented in CASTEP simulations are carried out. NVT (constant number of atoms N, volume V and temperature T) ensemble has been selected, Nose-Hoover thermostat method is used to control temperatures during the simulations, and external pressure is not applied. The simulation time step is 1 fs, and total simulation time is selected 1.5 ps, which is consistent with previous reports [38,39]. As shown in Fig. 6(a), only one H_2 molecule is away from each V atom because it is more weakly bound by the V atom, and other H_2 molecules are still strongly adsorbed around each V atom. There is no obvious structure deformation, indicating V atoms stably adsorbed on the PG surface. So, at the ambient temperature, six H_2 molecules can be adsorbed on both sides of V-PG with the gravimetric hydrogen storage capacity of 4.58 wt%. Fig. 6(b) describes the fluctuations of total energy as function of simulation time at 300 K, we can clearly see that there is no big fluctuation in curves, but only vibration in a very small range, which indicates the structure of H_2 molecules adsorbed on V-PG is stable in room temperature.

4. Conclusion

In summary, we have studied the electronic properties of V atoms adsorbed on PG and the adsorption ability of H_2 molecules on V-PG. A V atom is strongly adsorbed on the center of the C hexagon in the PG layer, but, two V atoms tend to aggregate with adjacent V atoms if they are initially placed in the same side of the PG unit cell. So, only one V atom should be adsorbed on the single side of the PG unit cell. The maximum number of adsorbed H_2 molecules around a V atom is four, but, only three H_2 molecules can be strongly adsorbed around each V atom by analyzing adsorption energies of H_2, which is consistent with the conclusion of analyzing charge density differences and partial densities of states. Two adsorption mechanisms contribute to the H_2 molecules: the polarization of the H_2 molecules under the electric field produced by the interaction between V and PG, and the orbital hybridization among H_2 molecules, V atoms and C atoms. At 300 K and without external pressure, ab initio MD simulation results show that six H_2 molecules can be adsorbed on both sides of V-PG unit cell with the gravimetric hydrogen storage capacity of 4.58 wt%, and the structure of H_2 molecules adsorbed on V-PG is stable, which indicates V-decorated PG can be used as a potential hydrogen storage medium at ambient conditions.

Declaration of interests

The authors declared that there is no conflict of interest.

Acknowledgements

The work is supported by the Natural Science Foundation of Gansu Province, China (Grant No. 17JR5RA123), the National Natural Science of Foundation of China (Grant No. 51562022) and the HongLiu first-class disciplines Development Program of Lanzhou University of Technology, China. We would like to give great thanks to Dr. Ma J. (Associate Editor for Nonlinear Dynamics) for useful discussions. We are also appreciative of Supercomputing Environment of Chinese Academy of Sciences.

Appendix A. Supplementary material

Supplementary data to this article can be found online at https://doi.org/10.1016/j.cplett.2019.04.026.

References

[1] P. Jena, Materials for hydrogen storage: past, present, and future, J. Phys. Chem. Lett. 2 (2011) 206–211.
[2] S. Nachimuthu, P.J. Lai, E.G. Leggesse, et al., A first principles study on boron doped graphene decorated by Ni-Ti-Mg atoms for enhanced hydrogen storage performance, Sci. Rep. 5 (2015) 16797.
[3] I. Cabria, M.J. Lopez, J.A. Alonso, Enhancement of hydrogen physisorption on graphene and carbon nanotubes by Li doping, J. Chem. Phys. 123 (2005) 204721.
[4] J.H. Liao, Y.J. Zhao, X.B. Yang, Controllable hydrogen adsorption and desorption by strain modulation on Ti decorated defective graphene, Int. J. Hydrogen Energy 40 (2015) 12063–12071.
[5] B. Panella, M. Hirscher, S. Roth, Hydrogen adsorption in different carbon nanostructures, Carbon 43 (2005) 2209–2214.
[6] F.D. Wang, F. Wang, N.N. Zhang, et al., High-capacity hydrogen storage of Na-decorated graphene with boron substitution: First-principles calculations, Chem. Phys. Lett. 555 (2013) 212–216.
[7] C. Ataca, E. Aktürk, S. Ciraci, et al., High-capacity hydrogen storage by metallized graphene, Appl. Phys. Lett. 93 (2008) 043123.
[8] I. Cabria, M.J. López, J.A. Alonso, Hydrogen storage in pure and Li-doped carbon nanopores: combined effects of concavity and doping, J. Chem. Phys. 128 (2008) 144704.
[9] C. Ataca, E. Aktürk, S. Ciraci, Hydrogen storage of calcium atoms adsorbed on graphene: first-principles plane wave calculations, Phys. Rev. B 79 (2009) 041406.
[10] T. Hussain, B. Pathak, M. Ramzan, et al., Calcium doped graphane as a hydrogen storage material, Appl. Phys. Lett. 100 (2012) 183902.
[11] C. Chen, J. Zhang, B. Zhang, et al., Hydrogen adsorption of Mg-doped graphene oxide: a first-principles study, J. Phys. Chem. C 117 (2013) 4337–4344.
[12] H. Lee, J. Ihm, M.L. Cohen, et al., Calcium-decorated graphene-based nanostructures for hydrogen storage, Nano Lett. 10 (2010) 793–798.
[13] E. Durgun, S. Ciraci, T. Yildirim, Functionalization of carbon-based nanostructures with light transition-metal atoms for hydrogen storage, Phys. Rev. B 77 (2008) 085405.
[14] H.P. Zhang, X.G. Luo, X.Y. Lin, et al., Density functional theory calculations of hydrogen adsorption on Ti-, Zn-, Zr-, Al-, and N-doped and intrinsic graphene sheets, Int. J. Hydrogen Energy 38 (2013) 14269–14275.
[15] O. Faye, J.A. Szpunar, An efficient way to suppress the competition between adsorption of H_2 and desorption of nH_2-Nb complex from graphene sheet: a promising approach to H_2 storage, J. Phys. Chem. C 122 (2018) 28506–28517.
[16] O. Faye, J.A. Szpunar, B. Szpunar, et al., Hydrogen adsorption and storage on palladium – functionalized graphene with NH-dopant: a first principles calculation, Appl. Surf. Sci. 392 (2017) 362–374.
[17] O. Faye, U. Eduok, J. Szpunar, et al., Hydrogen storage on bare Cu atom and Cu-functionalized boron-doped graphene: a first principles study, Int. J. Hydrogen Energy 42 (2017) 4233–4243.
[18] T. Zhang, C. Ling, Q. Xue, et al., The effect of oxygen molecule on the hydrogen storage process of Li-doped graphene, Chem. Phys. Lett. 599 (2014) 100–103.
[19] M. Bieri, M. Treier, J.M. Cai, et al., two-dimensional polymer synthesis with atomic precision, Chem. Commun. 6919–6922 (2009).
[20] A.J. Du, Z.H. Zhu, S.C. Smith, Multifunctional porous graphene for nanoelectronics and hydrogen storage: new properties revealed by first principle calculations, J. Am. Chem. Soc. 132 (2010) 2876–2877.
[21] M. Hatanaka, Band structures of porous graphenes, Chem. Phys. Lett. 488 (2010) 187–192.
[22] Z.M. Ao, S.X. Dou, Z.M. Xu, et al., Hydrogen storage in porous graphene with Al decoration, Int. J. Hydrogen Energy 39 (2014) 16244–16251.
[23] Z.M. Ao, F.M. Peeters, High-capacity hydrogen storage in Al-adsorbed graphene, Phys. Rev. B 81 (2010) 205406.
[24] P. Reunchan, S.H. Jhi, Metal-dispersed porous graphene for hydrogen storage, Appl. Phys. Lett. 98 (2011) 093103.
[25] S.H. Huang, L. miao, Y.J. Xiu, et al., Lithium-decorated oxidized porous graphene for hydrogen storage by first principles study, J. Appl. Phys. 112 (2012) 124312.
[26] R.F. Lu, D.W. Rao, Z.L. Lu, et al., Prominently improved hydrogen purification and dispersive metal binding for hydrogen storage by substitutional doping in porous graphene, J. Phys. Chem. C 116 (2012) 21291–21296.
[27] Y. Wang, Y. Ji, M. Li, et al., Li and Ca co-decorated carbon nitride nanostructures as high-capacity hydrogen storage media, J. Appl. Phys. 110 (2011) 094311.
[28] L.H. Yuan, Y.H. Chen, L. Kang, et al., First-principles investigation of hydrogen storage capacity of Y-decorated porous graphene, Appl. Surf. Sci. 399 (2017) 463–468.
[29] L.H. Yuan, L. Kang, Y.H. Chen, et al., Hydrogen storage capacity on Ti-decorated porous graphene: first-principles investigation, Appl. Surf. Sci. 434 (2018) 843–849.
[30] Y.H. Chen, J. Wang, L.H. Yuan, et al., Sc-decorated porous graphene for high-capacity hydrogen storage: first-principles calculations, Materials 10 (2017) 894.
[31] J. Sun, H.T. Wang, J.L. He, et al., Ab initio investigations of optical properties of the high-pressure phases of ZnO, Phys. Rev. B 71 (2005) 125132.
[32] J.P. Perdew, K. Burke, M. Ernzerhof, Generalized gradient approximation made simpl, Phys. Rev. Lett. 77 (1996) 3865.
[33] S. Grimme, Semiempirical GGA-type density functional constructed with a long-range dispersion correction, J. Comput. Chem. 27 (2006) 1787.
[34] D.W. Rao, R.F. Lu, Z.S. Meng, et al., Electronic properties and hydrogen storage application of designed porous nanotubes from a polyphenylene network, Int. J. Hydrogen Energy 39 (2014) 18966–18975.
[35] G. Brunetto, P.A.S. Autreto, L.D. Machado, et al., Nonzero gap two-dimensional carbon allotrope from porous graphene, J. Phys. Chem. C 116 (2012) 12810–12813.
[36] G.J. Kubas, Metal-dihydrogen and σ-bond coordination: the consummate extension of the Dewar-Chatt-Duncanson model for metal-olefin π bonding, J. Organomet. Chem. 635 (2001) 37–68.
[37] Y.L. Liu, L. Ren, Y. He, et al., Titanium-decorated graphene for high-capacity hydrogen storage studied by density functional simulations, J. Phys.: Condensed Matter 22 (2010) 445301.
[38] T. Yildirim, S. Ciraci, Titanium-decorated carbon nanotubes as a potential high-capacity hydrogen storage medium, Phys. Rev. Lett. 94 (2005) 175501.
[39] F.D. Wang, T. Zhang, X.Y. Hou, et al., Li-decorated porous graphene as a high-performance hydrogen storage material: a first-principles study, Int. J. Hydrogen Energy 42 (2017) 10099–10108.